Clinical, Cosmetic and Investigational Dermatology

Dovepress
Taylor & Francis Group

Open Access Full Text Article

ORIGINAL RESEARCH

Efficacy Evaluation of N-Acyl-Phytosphingosine Prepared from Marula Oil Derived Fatty Acids in Skin Barrier Repair

Zhongwang Liu, Huilin Zhu, Yuge Yang, Huailong Chang

Global Research and Development Center, Shanghai Chicmax Cosmetic Co., Ltd., Shanghai, People's Republic of China

Correspondence: Zhongwang Liu; Huailong Chang, Global Research and Development Center, Shanghai Chicmax Cosmetic Co. Ltd., 710 Yishan Road, Xuhui District, Shanghai, 200233, People's Republic of China, Tel +86 19821832201; +86 19916793872, Email 19111520005@fudan.edu.cn; huailongchang@alumni.hust.edu.cn

Purpose: This study aims to assess the efficacy of a novel N-acyl-phytosphingosine prepared from marula oil derived fatty acids (MO-CER NPs) in repairing impaired skin barrier function.

Patients and Methods: MO-CER NPs were synthesized from N-acyl-phytosphingosine using marula oil as a fatty acid source. Their effects on skin barrier improvement were compared with those of conventional C18-CER NP. A 28-day clinical trial involving 32 subjects was conducted to evaluate the efficacy of a topical cream containing 0.05% MO-CER NPs on barrier-compromised skin.

Results: Treatment with MO-CER NPs alleviated UVB-induced barrier damage as effectively as C18-CER NP, evidenced by increased expression of filaggrin and loricrin and reduced count of sunburn cells. Notably, MO-CER NPs showed superior anti-inflammatory activity. Furthermore, MO-CER NPs upregulated key genes involved in ceramide biosynthesis, keratinocyte proliferation, and differentiation. The clinical trial confirmed that topical application of 0.05% MO-CER NPs significantly improved barrier function by reducing transepidermal water loss and erythema, while increasing skin thickness and density.

Conclusion: MO-CER NPs demonstrated superior efficacy over conventional C18-CER NP in ameliorating skin barrier dysfunction and inflammation, highlighting its potential for improving barrier-compromised skin conditions.

Keywords: ceramides, marula oil, keratinocyte, inflammation, skin barrier

Introduction

The stratum corneum, the outermost layer of the skin, acts as a crucial interface between the human body and the external environment.[1] It maintains epidermal homeostasis through an organized intercellular lipid matrix.[1] Among these lipids, ceramides, a major subgroup of sphingolipids, constitute approximately 50% of intercellular lipids and mediate multiple critical physiological functions.[2] Structurally, ceramides localize to the extracellular spaces of the stratum corneum and upper epidermis, forming a protective barrier that prevents transepidermal water loss (TEWL) and protects against microbial invasion, chemical irritants, and mechanical stress.[3] Ceramides also function as key signaling molecules that regulate epidermal cell proliferation, differentiation, apoptosis, and skin immune responses.[4]

Dysregulation of ceramides levels and composition is strongly associated with various dermatological disorders.[1] In atopic dermatitis, dysregulated ceramide subtypes manifests as elevated concentrations of α-hydroxyacyl-sphingosine (CER AS) and N-acyl-sphingosine (CER NS), accompanied by reduced levels of N-acyl-phytosphingosine (CER NP).[3] These changes correlate with the altered expression of enzymes involved in CER and fatty acid synthesis, such as ceramide synthase (CerS3 and CerS4), stearoyl-CoA desaturase 1, and elongase 1.[5,6] Psoriasis is a chronic inflammatory skin disease characterized by erythematous and scaling plaques. It is accompanied by decreased levels of CER NP, elevated CER NS and reduced acyl fatty acid chain length.[3] These changes can be attributed to the abnormal expression of serine palmitoyl transferase (SPT) and CerS enzymes (CerS1-6).[7–10] Although

https://doi.org/10.2147/CCID.S586054
Received: 14 December 2025
Accepted: 13 February 2026
Published: 5 March 2026

healthy skin preserves barrier homeostasis through the synthesis of specific ceramide subtypes, this innate repair mechanism is undermined by environmental variations and the aging process.[3] For instance, tape-stripping analysis of volar forearms from 99 volunteers revealed that both saturated and unsaturated ceramide levels were lower in autumn and winter than in spring and summer,[11] correlating with increased TEWL.[12] Additionally, research focusing on menopause has demonstrated a significant reduction in total ceramide levels in the skin of post-menopausal women relative to their pre-menopausal counterparts.[13]

Given the critical role of ceramides in skin health, topical supplementation has emerged as a promising therapeutic approach.[14,15] CER NP is the most abundant ceramide subgroup in the lipid matrix of the human stratum corneum.[16] As a core component of the epidermal lipid bilayer, CER NP is essential for maintaining the structural integrity and normal barrier function of the stratum corneum.[17] Numerous studies have demonstrated the potent capacity of CER NP in repairing and restoring damaged skin barrier function, making it a particularly widely investigated and applied active ingredient in cosmetic research and product development.[18–20] Nevertheless, the development of next-generation CER NP-based therapeutics remains a central focus of dermatological research. Marula oil is a natural plant oil extracted from the fruit kernels of *Sclerocarya birrea* (commonly referred to as the Marula tree), distributed across southern African countries such as South Africa, Botswana, Zimbabwe, Mozambique, Zambia, and Namibia.[21] As a plant-derived oil widely used in cosmetics, marula oil has attracted growing attention due to its notable skin and hair benefits—including hydration, non-irritancy, and occlusive effects—and is now extensively incorporated into cosmetic formulations[21] Furthermore, growing evidence suggests that marula oil is abundant in monounsaturated fatty acids (predominantly oleic acid) and antioxidants, and also exhibits anti-inflammatory, anti-aging, and antioxidant properties.[22–24] Despite its fatty acid profile being similar to that of olive oil, it offers tenfold greater resistance to lipid oxidation.[25,26] Notably, the fatty acid chain lengths of marula oil (C14–C22) closely match those of human skin ceramides, making it an ideal precursor for synthesizing plant-derived CER NPs.[27]

This study sought to synthesize a novel N-acyl-phytosphingosine prepared from marula oil derived fatty acids (MO-CER NPs) and evaluate their efficiency in preserving skin barrier function in comparison to C18-CER NP. Using in vitro models, we compared the barrier repair effects of MO-CER NPs with conventional C18-CER NP. Additionally, a clinical trial was conducted to assess the efficacy of a MO-CER NPs-containing cream in improving skin barrier function.

Materials and Methods

Preparation of MO-CER NPs

MO-CER NPs were synthesized according to an established protocol with minor modifications.[28] Briefly, virgin organic marula oil (Sethic Innovations Labo, Guangzhou, China) was subjected to alkaline hydrolysis using potassium hydroxide, followed by acidification to pH 3. The fatty acids in marula oil were isolated through ethyl acetate extraction and concentrated via vacuum evaporation. Subsequently, the fatty acids were reacted with N, N′-dicyclohexylcarbodiimide and phytosphingosine (Shanghai Macklin Biochemical Technology Co., Ltd., Shanghai, China) under continuous stirring at room temperature until completion of the reaction. The crude product was purified by sequential filtration, solvent washing, and vacuum evaporation. Final characterization was conducted using high-performance liquid chromatography (HPLC) under chromatographic conditions.[28] For HPLC analysis, an ULTIMATE LP-C8 column (150 mm × 4.6 mm, 5 μm particle size, 300 Å pore size) was employed, with the column temperature maintained at 40°C. The mobile phase consisted of water and acetonitrile (20:80, v/v), delivered isocratically at a flow rate of 1.0 mL/min. The injection volume was 10 μL, and detection was performed at a wavelength of 202 nm. The total runtime for each analysis was 20 min. The ceremide standards used in this study, including N-oleoyl-phytosphingosine (t18:0-C18:1 NP), N-linoleoyl-phytosphingosine (t18:0-C18:2 NP), N-palmitoyl-phytosphingosine (t18:0-C16:0 NP), and N-stearoyl-phytosphingosine (t18:0-C18:0 NP), were provided by Chongqing Zhihe Bio-Pharmaceutical Co., Ltd. (Chongqing, China).

Cell Viability Assay

HaCaT cells (1.2×10^4 cells/well), provided by Guangdong BioCell Biotechnology (Guangdong, China), were seeded in 96-well plates containing Dulbecco's Modified Eagle's Medium (Gibco, Waltham, MA) and incubated at 37 °C in a 5% CO_2 incubator (Thermo Fisher, Waltham, MA) for 24 h prior to the assay. Cell viability was assessed using 3-(4,5-dimethylthiazol-2-yl)-2,5-diphenyltetrazolium bromide (MTT; Sigma-Aldrich, St. Louis, MO) assay. Briefly, HaCaT cells were treated with serially diluted MO-CE R NPs for 24 h, followed by the addition of 0.5 mg/mL MTT solution and incubation at 37 °C for 4 h. After removing the supernatant, 150 μL dimethyl sulfoxide (Sigma-Aldrich) was added to each well. Absorbance was measured at 490 nm using a microplate reader (BioTek Instruments, Winooski, VT). Relative cell viability was determined by setting the viability of the untreated control to 100%.

Treatment of 3D Reconstructed Human Epidermal Equivalents

A commercially available 3D reconstructed human epidermal equivalent, EpiKutis®, along with the corresponding culture media, was supplied by Guangdong BioCell Biotechnology. These 3D epidermal models were first allowed to recover for 24 h in 6-well plates. To investigate the repairing effects of MO-CER NPs on the epidermal barrier, the equivalents were first irradiated with ultraviolet B (UVB; Philips, Amsterdam, Netherlands) at an intensity of 600 mJ/cm^2 to induce damage to the skin barrier.[29] After UVB irradiation, the equivalents were topically treated with either 0.05% C18-CER NP (C18:0, Zhihe Bio-Pharmaceutical, Chongqing, China) or 0.05% MO-CER NPs for 24 h.

Immunofluorescence Staining

After treatment, the 3D epidermal equivalents were fixed in 4% paraformaldehyde for 24 h and embedded in paraffin. The embedded tissues were sectioned at 4 μm. The sections were then deparaffinized and rehydrated before staining with anti-filaggrin (1:500; Abcam, Cambridge, MA) or anti-loricrin (1:500; Abcam) antibodies and visualized with a fluorophore-conjugated secondary antibody. The stained sections were subsequently imaged using an Olympus BX43 microscope (Olympus Corporation, Tokyo, Japan), and the integral optical density of the filaggrin (FLG) - positive and loricrin (LOR)-positive signals within the delineated regions was quantified using Image-Pro Plus.

Sunburn Cell Counting

Paraformaldehyde-fixed paraffin-embedded tissue sections were stained with hematoxylin and eosin (H&E) following standard protocols. Histological assessment was carried out using an Olympus BX53 microscope (Olympus Corporation). Images were captured, and characteristic sunburn cells were identified and counted in the predesignated regions of interest.

Measurement of Inflammatory Cytokines

Conditioned medium was harvested after treating the epidermal equivalents with 0.05% C18-CER NP, or 0.05% MO-CER NPs, and stored at −80 °C for future use. Quantification of inflammatory cytokines were performed using commercial enzyme-linked immunosorbent assay (ELISA) kits for interleukin-1α (IL-1α; Abcam), interleukin-6 (IL-6; Abcam), tumor necrosis factor-α (TNF-α; Novus Biologicals, Littleton, CO), and prostaglandin E2 (PGE2; Enzo Life Sciences, Farmingdale, NY) according to the manufacturer's instructions.

Quantitative Real-Time PCR

HaCaT cells were seeded in 6-well plates at a density of 3×10^5 cells per well and cultured until they reached 50–60% confluency. Except for the blank control group, the cells were treated for 24 h with 2 mL of culture medium containing 0.01% C18-CER NP, or 0.01% MO-CER NPs. After one wash with phosphate-buffered saline (PBS), 2 mL of PBS was added to the cells, which were then irradiated with UVB at a dose of 30 mJ/cm.[30] Following the removal of PBS, the growth medium containing the corresponding compounds (0.01% C18-CER NP, or 0.01% MO-CER NPs) was replenished, and the cells were further incubated at 37 °C under 5% CO_2 for 24 h. At the end of the treatment, total RNA was extracted from the cells using an RNAiso Plus Kit and reverse-transcribed to cDNA. Quantitative real-time PCR (qPCR) was performed using a CFX96 Touch

Real-Time PCR Detection System (Bio-Rad, Hercules, CA). The primers used in this study are listed in Table 1. The relative expression of each gene was quantified using the $2^{-\Delta\Delta Ct}$ method with *ACTB* as the internal control.

Clinical Study

A double-blinded, single-center, pre-post controlled clinical trial (NCT07066150) was conducted at the Société Générale de Surveillance SA (SGS) test center in Qingdao, Shandong Province, China, from February 11 to March 21, 2025. The study was performed in accordance with the Declaration of Helsinki and approved by the Xi'an Beauty Clinical Ethics Committee (Ethical Review No. (01), 2025/02; 3 February 2025), which is an independent third-party ethical review institution. Written informed consent was obtained from all participants before initiating any trial-related procedures.

Healthy adult Chinese women aged 18–60 years with sensitive skin as screened for a positive lactic acid sting test were recruited according to the inclusion and exclusion criteria. Additional inclusion criteria were as follows: 1) TEWL

Table 1 List of Primers Used in the Current Study

Gene Name	Primer Pairs
KRT1	Forward: 5′-GGCAGACATGGGGATAGTGTGA-3′
	Reverse: 5′-GCTGCAAGTTGGAGATCTGCTT-3′
KRT10	Forward: 5′-TACAGTCCCAACTGGCCTTG-3′
	Reverse: 5′-GCACACAGTAGCGACCTTCT-3′
IVL	Forward: 5′-AGGCCAGGTCCAAGACATTCA-3′
	Reverse: 5′-CTGGTGCTCTACAGGAAGCAATAC-3′
TGM1	Forward: 5′-CACCCTCACCAATGTCGTCT-3′
	Reverse: 5′-GCTGTCCAAGCTGGCAATG-3′
CERS3	Forward: 5′-CGCAGACCTGTAACACCCT-3′
	Reverse: 5′-AGGCAAGATCAGCGTGCAAT-3′
SPT1	Forward: 5′-CTAGGAGAGCATGGCCGAGG-3′
	Reverse: 5′-GGCCGGAAAGTCGCTGAT-3′
PPARA	Forward: 5′-CCTGCAAGAAATGGGAAACATCC-3′
	Reverse: 5′-CGAAGCTGGTGAAAGCGTGT-3′
PPARGC1A	Forward: 5′-CTTCTCCAAAGCTGAAGTCCTCT-3′
	Reverse: 5′-CTTGGTGGAGTTATTGCCTTGTG-3′
SPHK1	Forward: 5′-ACACAAGGTGGGATTACCTGAC-3′
	Reverse: 5′-TCAGTGTCATAGGAGGGCTTC-3′
S1PR2	Forward: 5′-GCTCTGCCTTCATCACGCTCT-3′
	Reverse: 5′-AGCTCTTGTCGCTGCCATACA-3′
ACTB	Forward: 5′-CTGTTCCAGCCCTCCTTCAT-3′
	Reverse: 5′-CCTGATGTCAATGTCGCACTTC-3′

Abbreviations: KRT1, keratin1; KRT10, keratin1; IVL, involucrin; TGM1, transglutaminase 1; CERS3, ceramide synthase 3; SPT1, serine palmitoyltransferase 1; PPARA, peroxisome proliferator-activated receptor A; PPARGC1A, peroxisome proliferator-activated receptor gamma coactivator 1A; SPHK1, sphingosine kinase 1; S1PR2, sphingosine 1-phosphate receptor 2.

in one cheek area > 15 g/h/m^2; 2) Stratum corneum moisture content in at least one cheek area ≤ 50 C.U.; 3) visual erythema score of 3–6 in one cheek area, evaluated using a 0–9 scale with 0.5-point increments based on the SGS standard atlas. Subjects who 1) refused to sign the informed consent form; 2) refused to comply with the study protocol requirements; 3) participated in any other ongoing clinical trials; 4) used cosmetics or medications on the day of assessment/testing; 5) were pregnant or breastfeeding; 6) undertook medication/therapy during the study period; 7) had infectious skin diseases or atopic dermatitis; 8) had moles, telangiectasia (spider veins), or other skin abnormalities in the assessment/test area; 9) underwent systemic steroid therapy or phototherapy within 1 month prior to the evaluation/test; 10) used topical medications or specialized skincare products (eg, those claiming high moisturizing, repair, or soothing effects) on the test area within 2 weeks prior to evaluation/testing; 11) had lesions, visible marks, or abnormalities in the assessment/test area that may impede accurate measurements; 12) had a history of hypersensitivity or allergic reactions to cosmetics, medications, or general light exposure; or 13) had other conditions deemed ineligible for evaluation/testing by the principal investigator were excluded from the study. The participants were instructed to apply a cream containing 0.05% MO-CER NPs to their faces twice daily for 28 consecutive days. In addition to the beginning (D0) and end (D28) of the study, the participants were asked to visit the test center after applying the cream for 7 days (D7). During each visit, TEWL, skin hydration, *a** value, skin erythema, skin thickness, and skin density were assessed.

Statistical Analysis

For in vitro experiments, statistical analyses were conducted using one-way ANOVA followed by Dunnett's post hoc test or the Kruskal–Wallis test when the required assumptions were not met. For the clinical data, the differences were statistically analyzed using a two-tailed paired-sample *t*-test or non-parametric Wilcoxon signed-rank test, when appropriate. Differences were considered statistically significant at a threshold of $P < 0.05$.

Results

MO-CER NPs Exhibit Superior Potential in Enhancing Ceramide Synthesis and Keratinocyte Functions

In the present study, MO-CER NPs were composed of ceramides with variations in the length and saturation of the acyl chains which were inherited from marula oil. HPLC analysis showed that the main components of MO-CER NPs were *N*-oleoyl-phytosphingosine (t18:0-C18:1 NP, 69.27%), *N*-linoleoyl-phytosphingosine (t18:0-C18:2 NP, 8.81%), *N*-palmitoyl-phytosphingosine (t18:0-C16:0 NP, 8.12%), and *N*-stearoyl-phytosphingosine (t18:0-C18:0 NP, 4.61%) (Supplementary Figure S1, Table 2). Minor components, including *N*-linolenoyl-phytosphingosine (t18:0-C18:3 NP), *N*-lauroyl-phytosphingosine (t18:0-C12:0 NP), and *N*-myristoyl-phytosphingosine (t18:0-C14:0 NP), collectively accounted for 9.19% of the total CER NPs (Supplementary Figure S1, Table 2).

The MTT assay was performed to assess the cytotoxicity of the MO-CER NPs in HaCaT cells. No significant cytotoxicity was observed at concentrations up to 0.01% (w/w), with cell viability exceeding 90% after 24 h (Supplementary Figure S2). We first assessed the role of MO-CER NPs in inducing ceramide synthesis by measuring the mRNA expression levels of *CERS3* and *SPT1* in UVB-irradiated HaCaT cells. UVB exposure markedly downregulated *CERS3* and *SPT1* levels by 61.51% (Figure 1A) and 35.57% (Figure 1B), correspondingly, relative to untreated controls. Both MO-CER NPs and C18-CER NP significantly attenuated this effect (Figure 1). Notably, MO-

Table 2 Characterization of Marula oil and MO-CER NPs

Sample	Content According to Chain Length and Saturation (%)				
	C16:0	C18:0	C18:1	C18:2	Others
Marula oil	10-13	5-8	70-80	3-7	< 3
MO-CER NPs	8.12	4.61	69.27	8.81	9.19

https://doi.org/10.2147/CCID.S586054

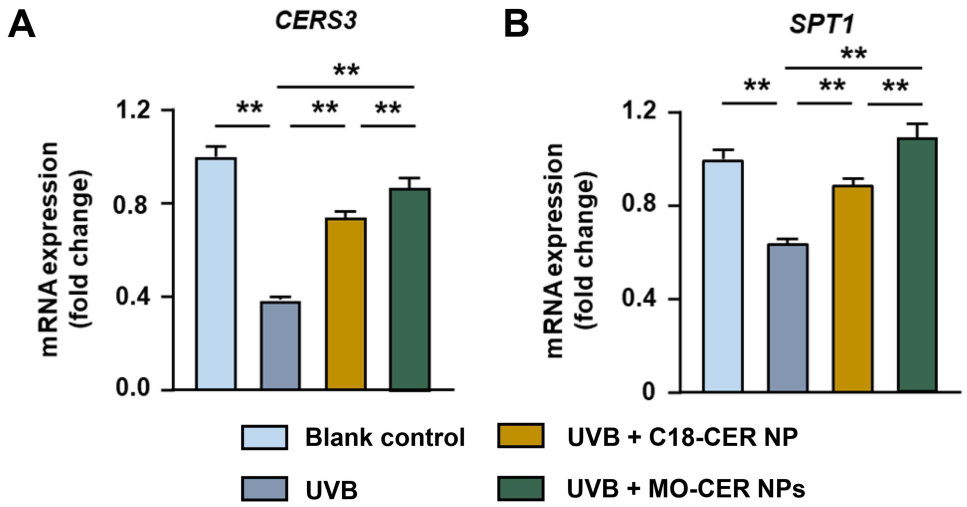

Figure 1 MO-CER NPs induced a more robust expression of genes related to ceramide biosynthesis compared to C18-CER NP. Relative expression of mRNA for (**A**) *CERS3*, (**B**) *SPT1* in HaCaT cells was quantified with qPCR. Data was presented as mean ± SD (n = 3, $^{**}P < 0.01$).

CER NPs induced a further increase, elevating *CERS3* and *SPT1* by 17.6% (Figure 1A) and 22.11% (Figure 1B), respectively, compared to C18-CER NP in UVB-damaged cells.

Given the positive role of C18-CER NP in promoting keratinocyte differentiation and proliferation, we compared the effects of MO-CER NPs by quantifying the expression of key markers, including KRT1, KRT10, IVL, and TGM1. Both CER NPs significantly counteracted UVB-induced suppression of *KRT1, KRT10, and TGM1* in HaCaT cells (Figure 2A, B and D). Strikingly, MO-CER NPs uniquely restored *IVL* expression in UVB-treated HaCaT cells (Figure 2C). Compared to C18-CER NP, MO-CER NPs further elevated the levels of *KRT10, IVL*, and *TGM1* by 26.5% (Figure 2B), 117.37% (Figure 2C), and 68.96% (Figure 2D), respectively.

MO-CER NPs Demonstrate Comparable Efficacy to C18-CER NPs in Ameliorating UVB-induced Skin Barrier Dysfunction

Based on previous skin toxicity evaluations in 3D epidermal models,[31] a 0.05% concentration of MO-CER NPs was selected for subsequent studies using 3D reconstructed human epidermal equivalents. In UVB-irradiated epidermal equivalents, both MO-CER NPs and C18-CER NP significantly enhanced skin barrier restoration compared with the damaged controls. Treatment with C18-CER and MO-CER NPs increased FLG expression by 294.95% (Figure 3A and B) and 320.58% (Figure 3A and B), and LOR by 214.4% (Figure 3A and C) and 223.48% (Figure 3A and C), correspondingly. Both CER NPs markedly reduced sunburn cell counts by 78.95% (Figure 3D and E) and 71.05% (Figure 3D and E), with no significant difference between them. Collectively, these findings indicate that both CER NPs potently ameliorate UVB-induced barrier damage by upregulating key barrier proteins and reducing epidermal injury.

MO-CER NPs Show a Greater Inhibition of the UVB-Induced Inflammatory Response

Ceramides serve not only as essential structural elements of the epidermal barrier but also as potent bioactive mediators that regulate immune homeostasis.[32] To assess the anti-inflammatory effects of MO-CER and C18-CER NP, we quantified cytokine levels via ELISA in UVB-irradiated 3D epidermal equivalents treated with these CERs. Following 24 h of treatment, MO-CER NPs, in contrast to C18-CER NP, significantly downregulated the levels of IL-1α, PGE2, and TNF-α by 21.34% (Figure 4A), 9.65% (Figure 4B) and 15.25% (Figure 4C), correspondingly, compared with UVB-irradiated controls. Additionally, the IL-6 levels in the culture medium of epidermal equivalents treated with MO-CER NPs and C18-CER NP were decreased by 25.51% (Figure 4D) and 19.09% (Figure 4D), respectively, relative to the UVB group.

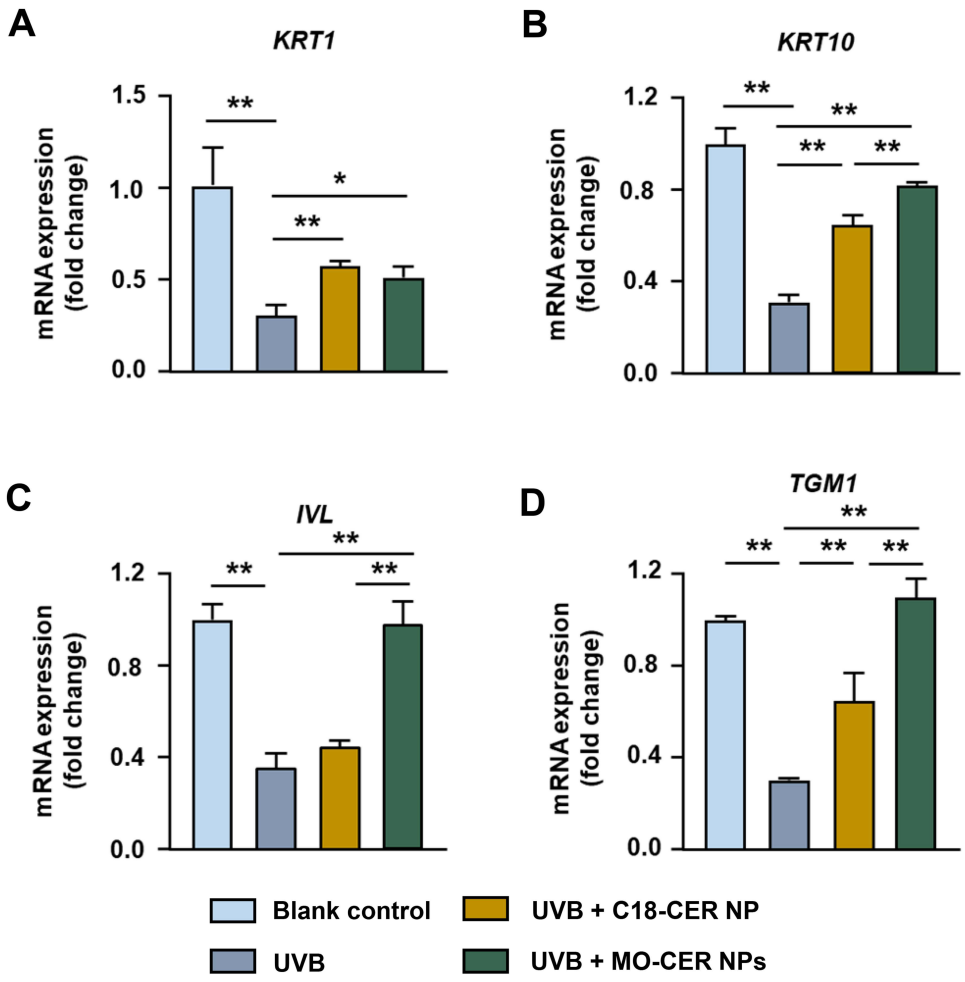

Figure 2 MO-CER NPs enhanced the mRNA expression of keratinocyte proliferation and differentiation markers relative to C18-CER NP. Relative expression of mRNA for (**A**) *KRT1*, (**B**) *KRT10*, (**C**) *IVL*, and (**D**) *TGM1* in HaCaT cells was quantified with qPCR. Data was presented as mean ± SD (n = 3, $^{**}P < 0.01$ and $^{*}P < 0.05$).

MO-CER NPs Enhance the Transcription of PPARα, PGC-1α, S1P and S1PR2

Because the peroxisome proliferator activated receptor α (PPARα)/PPARα coactivator 1α (PGC-1α) and sphingosine 1-phosphate (S1P)/sphingosine 1-phosphate receptor 2 (S1PR2) signaling pathways contribute to keratinocyte differentiation, proliferation, and cutaneous immune responses,[33,34] we also evaluated the differential capacity of C18-CER NP versus MO-CER NPs to activate these pathways in UVB-irradiated HaCaT cells. UVB significantly downregulated peroxisome proliferator-activated receptor A (*PPARA*, Figure 5A, 25.5%), peroxisome proliferator-activated receptor gamma coactivator 1A (*PPARGC1A*,Figure 5B, 43.56%), sphingosine kinase 1 (*SPHK1*, Figure 5C, 47.43%), and *S1PR2* (Figure 5D, 46.64%) compared to the untreated controls. Both CER NPs restored the mRNA levels of these four genes relative to those in UVB-treated cells (Figure 5). Compared with the UVB-treated group, C18-CER NP increased the expression of *PPARA, PPARGC1A, SPHK1*, and *S1PR2* by 10.68% (Figure 5A), 107.97% (Figure 5B), 48.57% (Figure 5C), and 78.19% (Figure 5D), respectively, whereas MO-CER NPs induced greater elevations, with increases of 39.01% (Figure 5A), 133.69% (Figure 5B), 78.99% (Figure 5C), and 148.41% (Figure 5D), correspondingly. Critically, MO-CER NPs enhanced activation compared with C18-CER NP, increasing *PPARA* (Figure 5A, 265.28%), *PPARGC1A* (Figure 5B, 23.82%), *SPHK1* (Figure 5C, 62.61%), and *S1PR2* (Figure 5D, 89.81%) expression beyond C18-CER NP-mediated restoration.

https://doi.org/10.2147/CCID.S586054

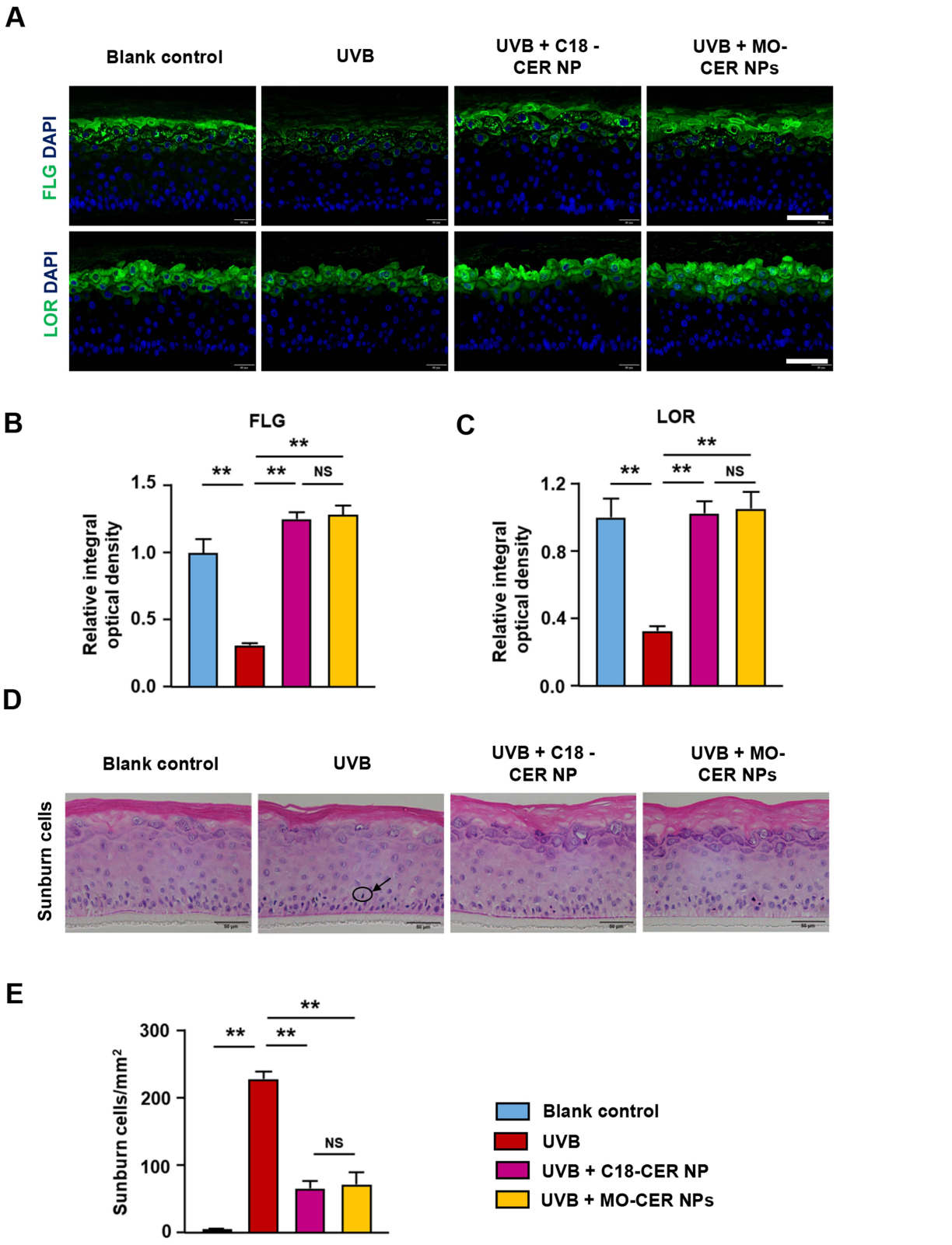

Figure 3 MO-CER NPs and C18-CER NP enhanced skin barrier repair and reduced sunburn cells in UVB-irradiated 3D epidermal models. (**A**) Representative images of FLG and LOR in the EpiKutis® 3D epidermal equivalents stained by immunofluorescence. Scale bar, 100 μm. (**B** and **C**) Quantification of FLG and LOR for each group. Data was presented as mean ± SD (n = 3, $^{**}P < 0.01$). (**D**) Representative images of sunburn cells in the EpiKutis® 3D epidermal equivalents stained by H&E. The arrow points to the sunburned cell. Scale bar, 50 μm. (**E**) Quantification of sunburn cells for each group. Data was presented as mean ± SD (n = 3, $^{**}P < 0.01$).

 https://doi.org/10.2147/CCID.S586054

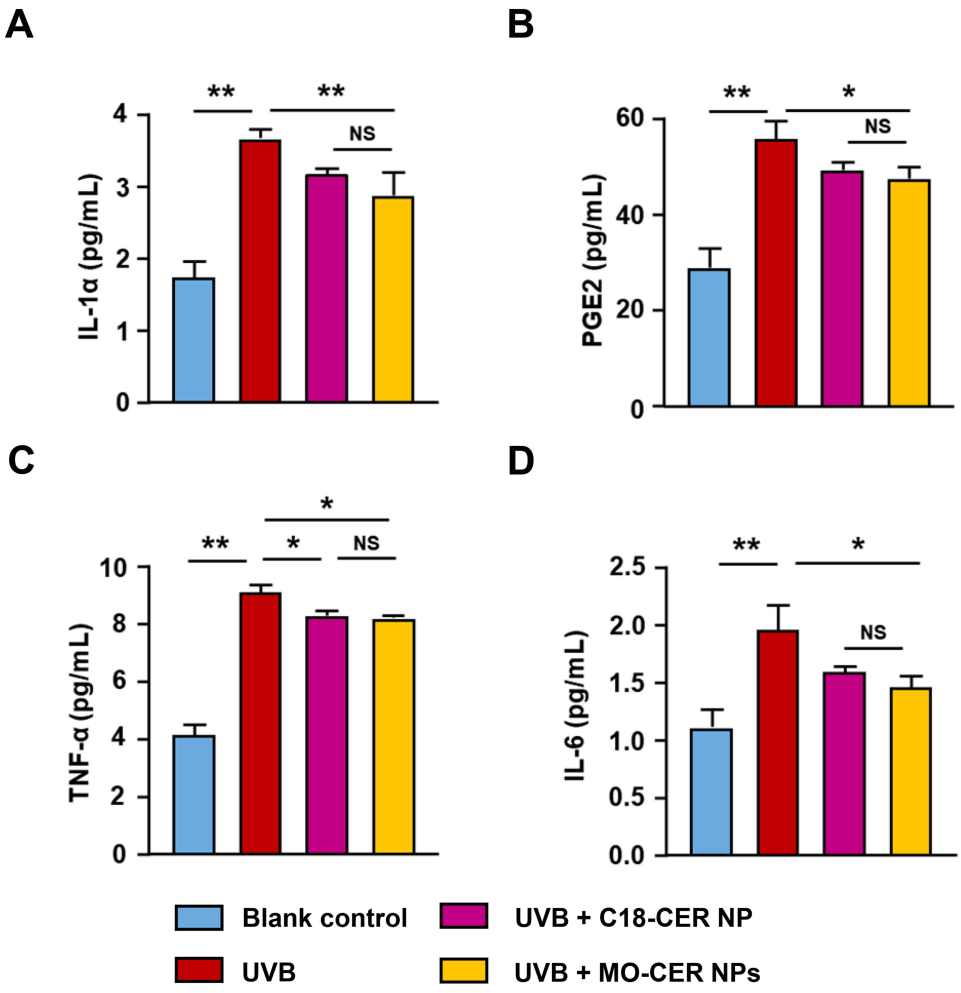

Figure 4 MO-CER NPs exhibited superior efficacy in inhibiting inflammatory cytokine secretion over C18-CER NP. The concentration of (**A**) IL-1α, (**B**) PGE2, (**C**) TNF-α, (**D**) IL-6 in the culture medium from 3D epidermal equivalents was quantified using ELISA. Data was presented as mean ± SD (n = 3, $^{**}P < 0.01$ and $^{*}P < 0.05$).

MO-CER NPs Ameliorate Skin Barrier Function in Human Subjects with Sensitive Skin

Building on the established barrier-restorative efficacy of 0.05% MO-CER NPs in 3D human epidermis models, we clinically assessed their safety and bioactivity in participants with sensitive skin. The participants were confirmed to have sensitive skin through lactic acid stinging testing with topical 0.05% MO-CER NPs cream applied twice daily. The formulation demonstrated excellent tolerability, with no treatment-emergent local or systemic adverse events during the study.

Instrumental measurements revealed significant improvements in TEWL and skin hydration at days 7 and 28 compared to day 0 (Figure 6A and B). Specifically, TEWL decreased by 3.72% (vs D0, Figure 6A) and 2.81% (vs D7, Figure 6A) at day 28, whereas skin water content increased by 10.19% (vs D0, Figure 6B) and 13.84% (vs D7, Figure 6B) at the same time points. Concomitant with enhanced moisturization, the a^* values and red area showed consistent reductions, with a^* values significantly decreased by 6.37% (Figure 6C and D) at day 7 and 6.92% (Figure 6C and D) at day 28 compared to D0. Similarly, the red area decreased by 8.64% (Figure 6C and E) and 9.68% (Figure 6C and E) at days 7 and 28, respectively. Importantly, skin thickness and density significantly increased by 2.59% (Figure 6F and G), and 10.97% (Figure 6F and H), respectively, on day 7 compared to day 0. By day 28, skin thickness and density had significantly increased by 1.46% (Figure 6F and G) and 3.57% (Figure 6F and H), respectively, compared to day 7.

https://doi.org/10.2147/CCID.S586054

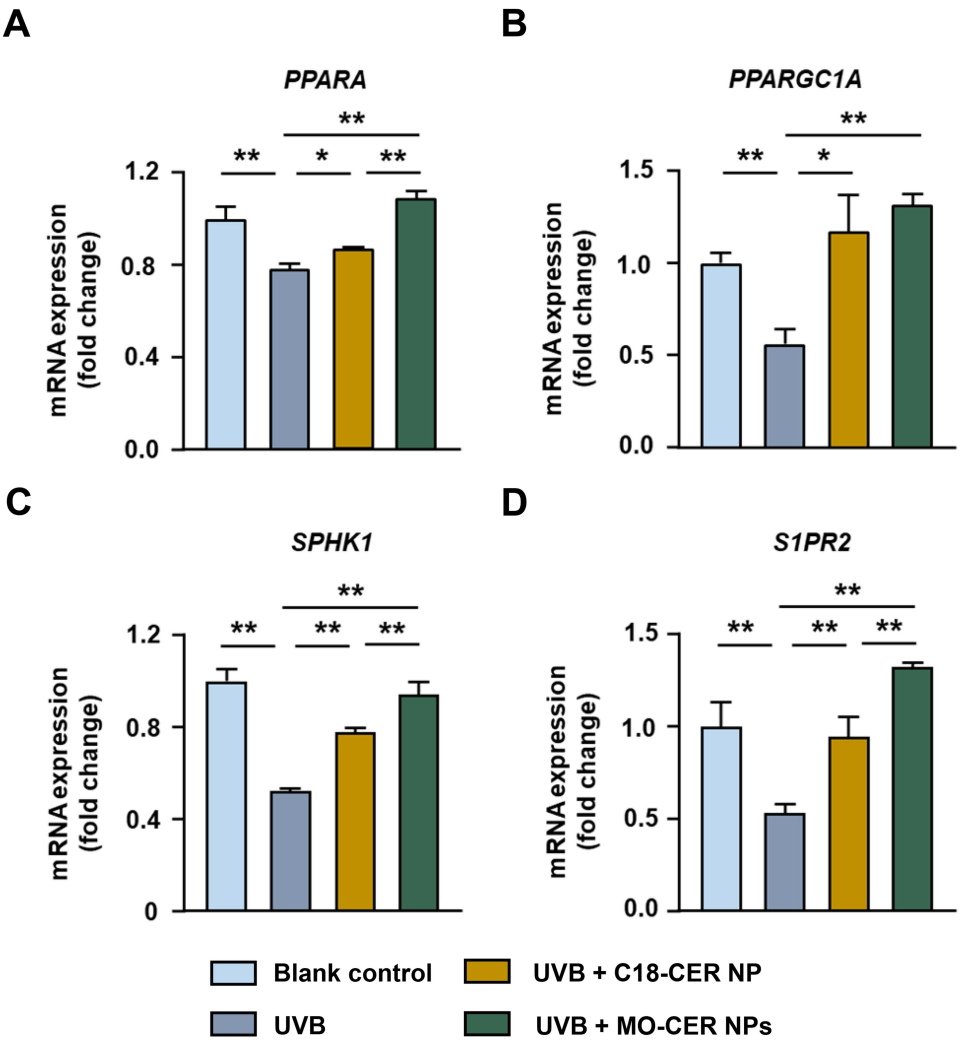

Figure 5 MO-CER NPs led to enhanced transcription of PPARα/PGC-1α and S1P/S1PR2 signaling pathways compared to C18-CER NP. Relative expression of mRNA for (**A**) *PPARA*, (**B**) *PPARGC1A*, (**C**) *SPHK1*, and (**D**) *SIPR2* in HaCaT cells was quantified with qPCR. Data was presented as mean ± SD (n = 3, $^{**}P < 0.01$ and $^{*}P < 0.05$).

Discussion

This study demonstrated that MO-CER NPs exert superior efficacy compared to conventional C18-CER NP in enhancing skin barrier function and mitigating inflammatory responses. Specifically, MO-CER NPs outperformed C18-CER NP in promoting keratinocyte differentiation and proliferation, increasing ceramide biosynthesis, and enhancing the transcription of the PPARα/PGC-1α and S1P/S1PR2 signaling pathways. Clinical findings further validated these advantages, showing significant improvements in the barrier function in participants with sensitive skin. Collectively, these results highlight MO-CER NPs as promising choice for repairing dermatological conditions characterized by barrier dysfunction.

Stratum corneum, characterized by its "brick-and-mortar" structure, relies heavily on the integrity of its intercellular lipid lamellae, where ceramides are the predominant component.[35,36] Disruptions in this architecture, as observed in atopic dermatitis, psoriasis, and photoaging, are strongly associated with reduced ceramide levels and altered subtype composition.[3,7] FLG organizes keratin filaments, contributes to natural moisturizing factors upon degradation, and reinforces the physical barrier,[37] whereas LOR, a major component of the cornified envelope, imparts mechanical resilience and desiccation resistance to the stratum corneum.[38] Our findings confirmed that both MO-CER NPs and C18-CER NP ameliorated UVB-induced barrier damage by upregulating FLG and LOR, two pivotal proteins in stratum corneum homeostasis. Notably, MO-CER NPs induced a more robust restoration of FLG and LOR expression than C18-CER NP in UV-irradiated 3D epidermal models. This superiority translated to functional improvements in clinical

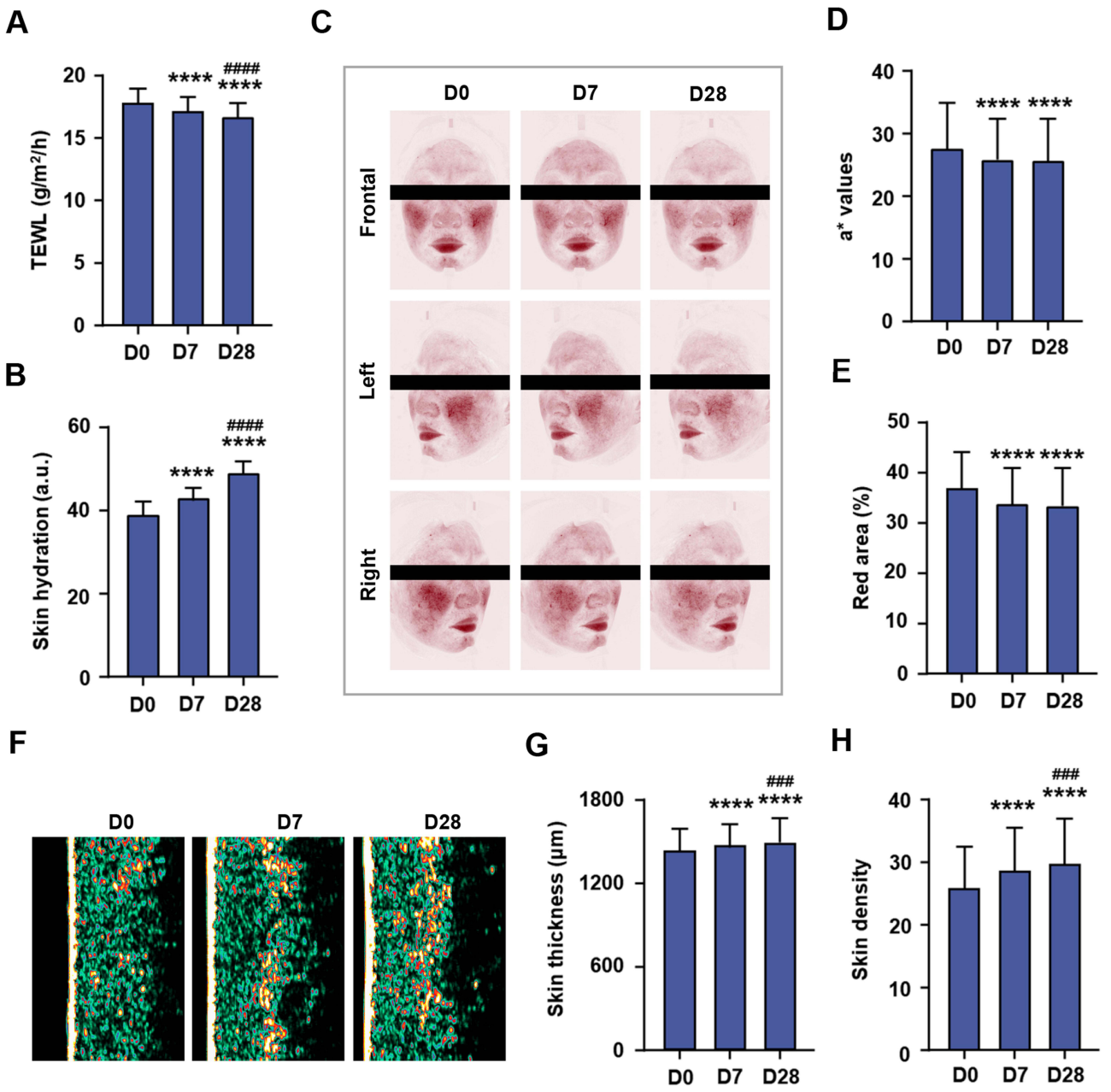

Figure 6 Application of a cream containing MO-CER NPs improved skin conditions in subjects with sensitive skin. (**A**) TEWL was measured by Tewameter®™ Hex at D0, D7, and D28. (**B**) Skin hydration was measured by Corneometer®CM825 at D0, D7, and D28. (**C**) Representative images of erythema area were captured by VISIA®-CR 5.0 at D0, D7, and D28. (**D** and **E**) Quantitative determinations of *a** values and red area at D0, D7, and D28. (**F**) Representative images of skin thickness and density were captured by DermaLab®Combo at D0, D7, and D28. (**G** and **H**) Quantitative determinations of skin thickness and density at D0, D7, and D28. Data was presented as mean ± SD (n = 32). ****$P < 0.0001$ compared to D0 (baseline); $^{\#\#\#}P < 0.001$ and $^{\#\#\#\#}P < 0.0001$ compared to D7.

Abbreviation: TEWL, trans-epidermal water loss.

settings, such as reduced TEWL and increased skin hydration, which is consistent with enhanced barrier integrity. Additionally, the observed increases in skin thickness and density following MO-CER NPs application align with previous reports that ceramide-containing formulations not only replenish lipids but also re-establish the structural coherence of the lipid matrix,[1,3,39] further supporting their role in rebuilding the stratum corneum architecture.

Beyond its structural integrity, the skin barrier relies on an immunological layer to maintain homeostasis.[40] Keratinocytes, as key sentinels, secrete pro-inflammatory cytokines (eg, IL-1α, IL-6, and TNF-α) and lipid mediators (eg, PGE2) in response to barrier disruption, amplifying inflammation and further impairing barrier function.[32,40] Our

https://doi.org/10.2147/CCID.S586054

results showed that MO-CER NPs exerted stronger inhibitory effects on these cytokines than C18-CER NP. This enhanced anti-inflammatory efficacy likely contributes to their superior barrier repair capacity, as reduced cytokine levels would mitigate immune-mediated damage to keratinocytes and lipid lamellae.

The mechanistic basis for this difference may lie in NPs' broader lipid profile of NPs: whereas C18-CER NP consist of a single fatty acid chain (C18:0), MO-CER NPs contain diverse chain lengths (C14-C22) and unsaturated fatty acids (eg, C18:1, 69.27%), which may interact more dynamically with immune signaling pathways. This aligns with recent evidence that plant-derived ceramides with heterogeneous fatty acid compositions better regulate skin homeostasis than single-chain synthetic ceramides.[41]

Endogenous ceramide synthesis is indispensable for barrier repair because exogenous supplementation alone cannot fully restore the dynamic balance of lipid subtypes.[42,43] Key enzymes involved in ceramide biosynthesis, including CERS3 and SPT1, were significantly upregulated by MO-CER NPs, with greater efficacy than that of C18-CER NP. CERS3 is critical for synthesizing very-long-chain ceramides essential for lamellar lipid organization,[5,17] whereas SPT1 initiates sphingolipid biosynthesis.[7] By enhancing the transcription of these enzymes, MO-CER NPs likely stimulate *de novo* ceramide production, complement exogenous supplementation, and support long-term barrier homeostasis.

Epidermal barrier repair also requires coordinated keratinocyte differentiation and proliferation, which orchestrate lipid biosynthesis and barrier protein expression.[44] MO-CER NPs upregulated genes encoding the keratinocyte markers KRT1 and KRT10 (proliferation), IVL (terminal differentiation), and TGM1 (cornified envelope formation). This suggests that MO-CER NPs not only replenish lipids but also promote the cellular processes necessary to rebuild epidermal layers.

The superior efficacy of MO-CER NPs is likely mediated by the enhanced activation of two key signaling pathways: PPARα/PGC-1α and S1P/S1PR2. PPARα, a nuclear receptor, regulates lipid metabolism and anti-inflammatory responses,[34,45] whereas its coactivator, PGC-1α, modulates energy metabolism and cellular stress resistance. The increased transcription of this pathway by MO-CER NPs may explain their ability to upregulate ceramide biosynthesis enzymes and suppress the secretion of inflammatory cytokines. The S1P/S1PR2 pathway, which is involved in keratinocyte survival, migration, and immune modulation,[33,46,47] was also strongly upregulated by MO-CER NPs. S1P protects keratinocytes from UVB-induced apoptosis and promotes wound healing;[46,47] thus, enhanced mRNA expression of S1P/S1PR2 may contribute to the reduced sunburn cell counts and improved epidermal histoarchitecture observed in the MO-CER NP-treated models. Together, these pathways integrate metabolic, proliferative, and immunomodulatory effects, providing a mechanistic framework for NPs' superior efficacy of MO-CER NPs.

Clinical validation in participants with sensitive skin confirmed the translational value of MO-CER NPs. Reductions in TEWL and erythema (a^* values, red area), and improvements in hydration, skin thickness, and density collectively demonstrate that the barrier repair mechanisms observed in vitro translate to tangible benefits in humans. The excellent tolerability of MO-CER NPs further supports their suitability for long-term use in sensitive or damaged skin. Although MO-CER NPs exhibit promising skin barrier repair potential, their practical cosmetic application is restricted by formulation compatibility with various cosmetic matrices, which requires further research.

Conclusion

MO-CER NPs may enhance skin barrier function through a coordinated mechanism involving key protein expression, lipid synthesis, keratinocyte differentiation, and activation of PPARα/PGC-1α and S1P/S1PR2 signaling pathways. Their superiority over C18-CER NP underscores the value of natural oil-derived ceramides with diverse fatty acid profiles, offering a novel therapeutic strategy for barrier-compromised skin conditions.

Data Sharing Statement

All data generated or analyzed during this study are presented within this article. Additional supporting information associated with this research can be obtained from the corresponding author, Zhongwang Liu, upon reasonable request.

Acknowledgments

The authors thank their colleagues at the Global R&D Center, Shanghai Chicmax Cosmetic Co., Ltd., for their invaluable support.

Disclosure

The authors report no conflicts of interest in this work.

References

1. Meckfessel MH, Brandt S. The structure, function, and importance of ceramides in skin and their use as therapeutic agents in skin-care products. *J Am Acad Dermatol*. 2014;71(1):177–184. doi:10.1016/j.jaad.2014.01.891
2. Burnett CL, Boyer IJ, Bergfeld WF, et al. Safety assessment of ceramides as used in cosmetics. *Int J Toxicol*. 2020;39(3_suppl):5s–25s. doi:10.1177/1091581820958692
3. Schild J, Kalvodová A, Zbytovská J, Farwick M, Pyko C. The role of ceramides in skin barrier function and the importance of their correct formulation for skincare applications. *Int J Cosmet Sci*. 2024;46(4):526–543.
4. Yong TL, Zaman R, Rehman N, Tan CK. Ceramides and skin health: new insights. *Exp Dermatol*. 2025;34(2):e70042. doi:10.1111/exd.70042
5. Ito S, Ishikawa J, Naoe A, et al. Ceramide synthase 4 is highly expressed in involved skin of patients with atopic dermatitis. *J Eur Acad Dermatol Venereol*. 2017;31(1):135–141. doi:10.1111/jdv.13777
6. Danso M, Boiten W, van Drongelen V, et al. Altered expression of epidermal lipid bio-synthesis enzymes in atopic dermatitis skin is accompanied by changes in stratum corneum lipid composition. *J Dermatol Sci*. 2017;88(1):57–66. doi:10.1016/j.jdermsci.2017.05.005
7. Motta S, Monti M, Sesana S, Caputo R, Carelli S, Ghidoni R. Ceramide composition of the psoriatic scale. *Biochim Biophys Acta*. 1993;1182 (2):147–151. doi:10.1016/0925-4439(93)90135-N
8. Checa A, Xu N, Sar DG, Haeggström JZ, Ståhle M, Wheelock CE. Circulating levels of sphingosine-1-phosphate are elevated in severe, but not mild psoriasis and are unresponsive to anti-TNF-α treatment. *Sci Rep*. 2015;5:12017. doi:10.1038/srep12017
9. Moon SH, Kim JY, Song EH, Shin MK, Cho YH, Kim NI. Altered levels of sphingosine and sphinganine in psoriatic epidermis. *Ann Dermatol*. 2013;25(3):321–326. doi:10.5021/ad.2013.25.3.321
10. Tawada C, Kanoh H, Nakamura M, et al. Interferon-γ decreases ceramides with long-chain fatty acids: possible involvement in atopic dermatitis and psoriasis. *J Invest Dermatol*. 2014;134(3):712–718.
11. Rogers J, Harding C, Mayo A, Banks J, Rawlings A. Stratum corneum lipids: the effect of ageing and the seasons. *Arch Dermatol Res*. 1996;288 (12):765–770.
12. Pappas A, Kendall AC, Brownbridge LC, Batchvarova N, Nicolaou A. Seasonal changes in epidermal ceramides are linked to impaired barrier function in acne patients. *Exp Dermatol*. 2018;27(8):833–836.
13. Mellody KT, Kendall AC, Wray JR, et al. Influence of menopause and hormone replacement therapy on epidermal ageing and skin biomechanical function. *J Eur Acad Dermatol Venereol*. 2022;36(7):e576–e580.
14. Choi MJ, Maibach HI. Role of ceramides in barrier function of healthy and diseased skin. *Am J Clin Dermatol*. 2005;6(4):215–223.
15. Coderch L, López O, de la Maza A, Parra JL. Ceramides and skin function. *Am J Clin Dermatol*. 2003;4(2):107–129.
16. Reuter M, Joseph E, Lian G, Lunter DJ. Presence of different ceramide species modulates barrier function and structure of stratum corneum lipid membranes: insights from molecular dynamics simulations. *Mol Pharm*. 2025;22(7):4280–4292. doi:10.1021/acs.molpharmaceut.5c00580
17. Breiden B, Sandhoff K. The role of sphingolipid metabolism in cutaneous permeability barrier formation. *Biochim Biophys Acta*. 2014;1841 (3):441–452.
18. Lee JY, Jeon S, Han S, Liu KH, Cho Y, Kim KP. Positive correlation of triacylglycerols with increased chain length and unsaturation with ω-O-acylceramide and ceramide-NP as well as acidic pH in the skin surface of healthy Korean adults. *Metabolites*. 2022;13(1):31. doi:10.3390/metabo13010031
19. Su Z, Zheng Y, Yi J, Lai W, Ye C. The effectiveness and safety of a skin care product with centella asiatica leaf extract, ceramide NP, and panthenol in subjects with sensitive skin: a prospective, observational study. *J Cosmet Dermatol*. 2025;24(7):e70324. doi:10.1111/jocd.70324
20. Bektay H Ş, Sağıroğlu AA, Bozali K, Güler EM, Güngör S. The design and optimization of ceramide NP-loaded liposomes to restore the skin barrier. *Pharmaceutics*. 2023;15(12).
21. Komane B, Vermaak I, Summers B, Viljoen A. Safety and efficacy of Sclerocarya birrea (A.Rich.) Hochst (Marula) oil: a clinical perspective. *J Ethnopharmacol*. 2015;176:327–335. doi:10.1016/j.jep.2015.10.037
22. Mariod AA, Abdelwahab SI. Sclerocarya birrea (Marula), An African tree of nutritional and medicinal uses: a review. *Food Reviews International*. 2012;28(4):375–388.
23. Deyama T, Nishibe S, Nakazawa Y. Constituents and pharmacological effects of Eucommia and Siberian ginseng. *Acta Pharmacol Sin*. 2001;22 (12):1057–1070.
24. Alshaman R, Qushawy M, Mokhtar HI, et al. Marula oil nanoemulsion improves motor function in experimental parkinsonism via mitigation of inflammation and oxidative stress. *Front Pharmacol*. 2023;14:1293306. doi:10.3389/fphar.2023.1293306
25. Mariod AA, Matthäus B, Hussein IH. Antioxidant properties of methanolic extracts from different parts of Sclerocarya birrea. *International Journal of Food Science & Technology*. 2008;43(5):921–926. doi:10.1111/j.1365-2621.2007.01543.x
26. Robinson E, Lukman A, Bello A. Investigation of extracted Sclerocarya birrea seed oil as a bioenergy resource for compression ignition engines. *International Journal of Agricultural & Biological Engineering*. 2012;5(3).
27. Mashau ME, Kgatla TE, Makhado MV, Mikasi MS, Ramashia SE. Nutritional composition, polyphenolic compounds and biological activities of marula fruit (Sclerocarya birrea) with its potential food applications: a review. *International Journal of Food Properties*. 2022;25(1):1549–1575. doi:10.1080/10942912.2022.2064491
28. Choi HK, Hwang K, Hong YD, et al. Ceramide NPs derived from natural oils of Korean traditional plants enhance skin barrier functions and stimulate expressions of genes for epidermal homeostasis. *J Cosmet Dermatol*. 2022;21(10):4931–4941. doi:10.1111/jocd.14905
29. Yuan M, Hu L, Zhu C, et al. Comparison and assessment of anti-inflammatory and antioxidant capacity between EGCG and phosphatidylcholine-encapsulated EGCG. *J Cosmet Dermatol*. 2025;24(1):e16628. doi:10.1111/jocd.16628
30. Lee HR, Yang JH, Lee JH, et al. Protective effect of castanopsis sieboldii extract against UVB-induced photodamage in keratinocytes. *Molecules*. 2023;28(6).

31. Chen L, Wu M, Jiang S, et al. Skin toxicity assessment of silver nanoparticles in a 3D epidermal model compared to 2D keratinocytes. *Int J Nanomedicine*. 2019;14:9707–9719. doi:10.2147/IJN.S225451
32. Li Q, Fang H, Dang E, Wang G. The role of ceramides in skin homeostasis and inflammatory skin diseases. *J Dermatol Sci*. 2020;97(1):2–8. doi:10.1016/j.jdermsci.2019.12.002
33. Masuda-Kuroki K, Di Nardo A. Sphingosine 1-phosphate signaling at the skin barrier interface. *Biology*. 2022;11(6):809. doi:10.3390/biology11060809
34. Kauppinen A, Suuronen T, Ojala J, Kaarniranta K, Salminen A. Antagonistic crosstalk between NF-κB and SIRT1 in the regulation of inflammation and metabolic disorders. *Cell Signal*. 2013;25(10):1939–1948.
35. Elias PM. Epidermal lipids, barrier function, and desquamation. *J Invest Dermatol*. 1983;80(1 Suppl):44s–49s. doi:10.1038/jid.1983.12
36. Elias PM, Menon GK. Structural and lipid biochemical correlates of the epidermal permeability barrier. *Adv Lipid Res*. 1991;24:1–26.
37. Rajkumar J, Chandan N, Lio P, Shi V. The skin barrier and moisturization: function, disruption, and mechanisms of repair. *Skin Pharmacol Physiol*. 2023;36(4):174–185. doi:10.1159/000534136
38. Ishitsuka Y, Roop DR. Loricrin: past, present, and future. *Int J Mol Sci*. 2020;21(7).
39. Kahraman E, Kaykın M, Şahin Bektay H, Güngör S. Recent advances on topical application of ceramides to restore barrier function of skin. *Cosmetics*. 2019;6(3):52.
40. Strugar TL, Kuo A, Seité S, Lin M, Lio P. Connecting the dots: from skin barrier dysfunction to allergic sensitization, and the role of moisturizers in repairing the skin barrier. *J Drugs Dermatol*. 2019;18(6):581.
41. Oh MJ, Cho YH, Cha SY, et al. Novel phytoceramides containing fatty acids of diverse chain lengths are better than a single C18-ceramide N-stearoyl phytosphingosine to improve the physiological properties of human stratum corneum. *Clin Cosmet Investig Dermatol*. 2017;10:363–371. doi:10.2147/CCID.S143591
42. Berkers T, Visscher D, Gooris GS, Bouwstra JA. Topically applied ceramides interact with the stratum corneum lipid matrix in compromised ex vivo skin. *Pharm Res*. 2018;35(3):48. doi:10.1007/s11095-017-2288-y
43. Ishida K, Takahashi A, Bito K, Draelos Z, Imokawa G. Treatment with synthetic pseudoceramide improves atopic skin, switching the ceramide profile to a healthy skin phenotype. *J Invest Dermatol*. 2020;140(9):1762–1770.e1768.
44. Man MQ, Wakefield JS, Mauro TM, Elias PM. Role of nitric oxide in regulating epidermal permeability barrier function. *Exp Dermatol*. 2022;31(3):290–298. doi:10.1111/exd.14470
45. Kippenberger S, Grundmann-Kollmann M, Simon S, et al. Activators of peroxisome proliferator-activated receptors protect human skin from ultraviolet-B-light-induced inflammation. *Journal of Investigative Dermatology*. 2001;117(6):1430–1436. doi:10.1046/j.0022-202x.2001.01537.x
46. Uchida Y, Houben E, Park K, et al. Hydrolytic pathway protects against ceramide-induced apoptosis in keratinocytes exposed to UVB. *J Invest Dermatol*. 2010;130(10):2472–2480. doi:10.1038/jid.2010.153
47. Moriue T, Igarashi J, Yoneda K, et al. Sphingosine 1-phosphate attenuates peroxide-induced apoptosis in HaCaT cells cultured in vitro. *Clin Exp Dermatol*. 2013;38(6):638–645. doi:10.1111/ced.12037